CrossMark

J. Fluid Mech. (2018), *vol.* 846, *pp.* 686–710. © Cambridge University Press 2018
doi:10.1017/jfm.2018.291

A second-order continuum theory of fluids

S. Paolucci[1],† and C. Paolucci[2]

[1]Aerospace & Mechanical Engineering, University of Notre Dame, Notre Dame, IN 46556, USA

[2]Chemical & Biomolecular Engineering, University of Notre Dame, Notre Dame, IN 46556, USA

(Received 31 October 2017; revised 23 March 2018; accepted 2 April 2018;
first published online 9 May 2018)

We use continuum conservation equations in conjunction with the entropy inequality to obtain a theoretical model that is accurate for hypersonic flows. This is accomplished by extending the constitutive equations to second order in strain rate and gradients of density and temperature. The accuracy of the extended theory is demonstrated by computing the shock structure in argon and nitrogen gases over a large range of Mach numbers. The solutions indicate that our constitutive equations are more accurate than the classical linear ones and are also more robust and accurate than equations obtained through expansions of the Boltzmann equation or equations arising from diffusion of volume arguments.

Key words: compressible flows, mathematical foundations, shock waves

1. Introduction

In engineering applications the thickness of the shock structure is often negligibly small in comparison with the characteristic dimension, so engineers are well satisfied with the Rankine–Hugoniot theory. However, the computation of the shock structure at large Mach numbers is of much interest in hypersonic flows (see Landau & Lifshitz 1959), particularly when additional physical phenomena need to be considered (such as chemistry).

The shock structure based on the Navier–Stokes–Fourier (NSF) equations has been well characterized (Morduchow & Libby 1949; von Mises 1950; Gilbarg 1951; Ludford 1951; Gilbarg & Paolucci 1953; Khonkin & Orlov 1993). In addition, a number of experimental studies have provided measurements of the shock structure over varying Mach number ranges (Sherman 1955; Linzer & Hornig 1963; Camac 1965; Russell 1965; Schultz-Grunow & Frohn 1965; Robben & Talbot 1966; Schmidt 1969; Rieutord 1970; Garen, Synofzik & Frohn 1974). In particular, accurate density measurements have been carried out in argon and nitrogen shock waves for a large Mach number range by Alsmeyer (1976). Subsequently, it is well known that the NSF equations do not represent the shock structure well even at moderate Mach numbers (see Gilbarg & Paolucci 1953; Liepmann, Narasimha & Chahine 1962; Alsmeyer 1976); the shock layer thickness is predicted to be too small compared to experiments, particularly at intermediate Mach numbers. In figure 1 the inverse shock thickness as a function of the upstream Mach number predicted by the NSF theory

† Email address for correspondence: paolucci@nd.edu

https://doi.org/10.1017/jfm.2018.291 Published online by Cambridge University Press

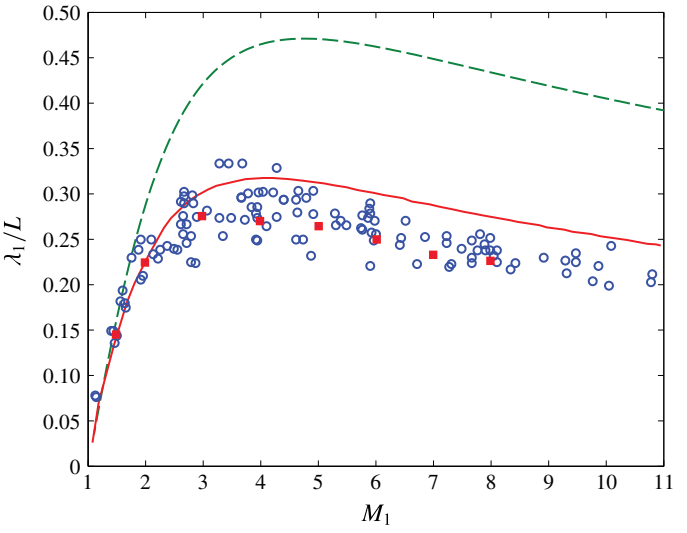


FIGURE 1. (Colour online) Inverse shock thickness, λ_1/L, as a function of upstream Mach number, M_1, for argon gas: ○, experimental results of Linzer & Hornig (1963), Camac (1965), Russell (1965), Schultz-Grunow & Frohn (1965), Robben & Talbot (1966), Schmidt (1969), Rieutord (1970), Garen *et al.* (1974) and Alsmeyer (1976); – – –, NSF theory; ■, direct simulation Monte Carlo results of Bird (1970); ——, theoretical results of Lumpkin & Chapman (1992), Woods (1993) and Reese *et al.* (1995).

(and by a number of other theories discussed below) is compared with experimental results (open circles). As can be observed, values obtained from the NSF equations differ significantly from the experimental measurements for Mach numbers larger than approximately 1.5.

The NSF equations represent a continuum theory based on linear constitutive relations between thermodynamic forces and fluxes (note that in general the Stokes assumption regarding bulk viscosity is not assumed). In a strong shock wave, the forces are large and the failure of the NSF equations could be attributed to deviations from the linear Newtonian and Fourier laws or to a mean free path too large for the continuum assumption to be accurate. Subsequently, the computation of the shock structure, particularly at the large Mach numbers encountered in hypersonic flows, has provided an excellent opportunity to find extended theories that would remedy this discrepancy.

The generally accepted parameter which indicates the extent to which a local region of flowing gas is in thermodynamic equilibrium is the Knudsen number, $Kn = \lambda/L \propto M/Re$, where λ is the mean free path of the gas molecules, L is a characteristic length of the flow system, $M = u/c$ is the flow Mach number with u the flow speed and c the speed of sound and $Re = \rho\, u\, L/\mu$ is the Reynolds number with ρ the mass density and μ the dynamic viscosity. If Kn is less than 10^{-3}, the gas can be assumed to undergo a large number of collisions over the typical length scale, and the conventional NSF equations are an appropriate model. Difficulties appear when Kn rises, either due to the low density of the gas (which makes the mean free path larger) or due to regions of high local gradients, such as in the shock structure. The situation becomes even more problematic as Kn rises to the range 0.1–1. This is called the 'transition–continuum regime' and it lies between the extremes of the continuum and

https://doi.org/10.1017/jfm.2018.291 Published online by Cambridge University Press

free molecular regimes. The range of use of the continuum–equilibrium assumption is therefore clearly limited, with the applicability of the classical NSF equations (with standard no-slip boundary conditions) confined to cases where $Kn \lesssim 0.01$, typically. The flow in the shock layer is far from being in local thermodynamic equilibrium, typically $Kn = 0.2$–0.3, i.e. very much within the intermediate-Kn regime.

Extended, or modified, hydrodynamics attempts to increase the range of applicability of the continuum–equilibrium fluid model into the transition–continuum regime where $0.01 \lesssim Kn \lesssim 1$. Since the NSF equations perform poorly at these values of Kn, the shock structure problem is particularly well suited for testing extended hydrodynamic models. (In passing, it should be noted that the linear NSF theory has been extended in liquids when dealing with what we call viscoelastic materials.)

Numerous higher-order continuum-fluid equation sets have been proposed for flows that depart from quasi thermodynamic equilibrium, mostly derived from the fundamental Boltzmann equation using different approaches (Thomas 1944; Liepmann *et al.* 1962). In its most basic form, the Boltzmann equation describes the evolution of a system of monatomic gas molecules, assuming molecular chaos and that only binary inter-molecular collisions occur (i.e. the gas needs to be dilute, although there are potential modifications which could allow for multiple collisions typical of dense gases). All such theories discussed below are limited to monatomic gases. The classical approach is the Chapman–Enskog technique (based on a series expansion in Kn) which determines a hierarchy of approximate solutions to the Boltzmann equation. The approach is limited by the convergence of the series ($Kn \lesssim 0.3$). The first term in the series results in the stress tensor equal to the pressure and the heat flux being zero (Euler equations). The first two terms in the series result in the linear constitutive equations associated with the NSF equations. The first three terms (second order in Kn) provide a complicated set of constitutive equations known as the Burnett equations (Chapman & Cowling 1970), which are presumed to extend the validity of the continuum model for flows at higher Kn than the NSF equations. Other similar second-order formulations include Grad's 13 moment (Grad 1949, 1952), reduced Burnett (Lumpkin & Chapman 1992), BGK-Burnett (Bhatnagar–Gross–Krook/Burnett) (Balakrishnan 2004), regularized Burnett and regularized Grad's 13 moment (Jin & Slemrod 2001; Struchtrup & Torrilhon 2003) and Woods (Woods 1983, 1993; Reese *et al.* 1995) equations. This is not an exhaustive list, but includes the most commonly used and cited. Balakrishnan & Agarwal (1999) provide a comparative study of second-order kinetic formulations applied to the shock structure problem. Most of these theories amount to adding, removing or modifying in an *ad hoc* fashion different terms in the Burnett equations or variants thereof. The leading reason for such modifications is that they are all plagued by numerical and physical instabilities and, in many cases, produce non-physical flow predictions. For example, Grad's 13-moment theory provides no continuous shock structure beyond $M = 1.65$. Similar to Grad's theory of moments, Weiss and others (Liu & Salvador 1990; Weiss 1995; Taniguchi *et al.* 2014*a*,*b*) extend the theory from 13 to 21 moments for densities of momentum and energy fluxes. Depending on the number of moments, there is a critical Mach number beyond which there are no solutions. The critical Mach number depends on the number of moments; it is 1.65 for 13 moments and 1.887 for 21 moments. We note that the result shown in figure 1 corresponds to that of Reese *et al.* (1995) obtained by *ad hoc* alteration and deletion of terms giving rise to non-physical effects in modified Barnett equations. The explanation of problems with stability may have been provided by Comeaux, Chapman & MacCormack (1995) who showed that the Burnett equations can violate the second law of thermodynamics.

https://doi.org/10.1017/jfm.2018.291 Published online by Cambridge University Press

Direct simulation Monte Carlo (DSMC) and molecular dynamics (MD) have also been used to obtain the shock structure (Bird 1970; Salomons & Mareschal 1992). As shown in figure 1, the DSMC results, obtained by using a simple repulsive intermolecular force law, show very good agreement with the experimental results over the large Mach number range. However, the large number of molecules required to accurately simulate the continuum–transition regime makes the DSMC technique prohibitively expensive with regard to computational cost and limits its applicability to simulations of flows in simple geometries.

It is noted that there have been extensions to the NSF theory in a variety of directions. In kinetic theory, there are works that consider polyatomic gases (Brau 1967; She & Sather 1967). In continuum theory, the most prominent extensions have been in the area of non-Newtonian and viscoelastic fluids (Coleman & Noll 1961; Coleman, Markovitz & Noll 1966). There have also been many works that consider fluids that can sustain internal spin under the rubric of micropolar or couple stress, but they all fall under the general micromorphic theory of Eringen (1999, 2001). A noteworthy extension is also that of Chen (2013) where the rate of temperature is accounted for in the formulation of the constitutive theory. Lastly, we note that Brenner (2005*a*,*b*) proposed modifications of the NSF equations based on a diffusion of volume argument which would be significant for flows with large density gradients. Greenshields & Reese (2007) modified Brenner's equations by introducing an additional physical parameter, the volume diffusivity. They applied their modified equations to the solutions of the steady shock wave as a test, and computed the structure in the Mach number range of 1–12. They also encountered instabilities in the solutions. Nevertheless, they were able to 'adjust' the equations to obtain somewhat better solutions than NSF equations with the addition of two terms.

In this work we use standard continuum theory to extend the constitutive equations. In § 2 we write the governing continuum balance equations for mass, linear momentum and energy, along with the entropy inequality representing the second law of thermodynamics. In § 3 we extend the constitutive equations necessitated by these equations to second order, not in Knudsen number, but in strain rate and gradients of density and temperature. We also discuss related equations of state. In § 4 we write the one-dimensional form of the governing equations relevant to the shock structure problem. The results for argon and nitrogen are presented in § 5. In § 6 we compare the new constitutive equations with those obtained through the Chapman–Enskog expansion and discuss the advantages of the extended model derived in the present work.

2. Governing equations

Ignoring external sources of momentum and energy, and assuming sufficient material smoothness, the fundamental local laws of conservation of mass, linear momentum and energy are given by

$$\dot{\rho} + \rho \operatorname{div} \boldsymbol{v} = 0, \tag{2.1}$$

$$\rho\, \dot{\boldsymbol{v}} - \operatorname{div} \boldsymbol{\sigma} = \boldsymbol{0}, \tag{2.2}$$

$$\rho\, \dot{e} - \Phi + \operatorname{div} \boldsymbol{q} = 0, \tag{2.3}$$

where a superposed dot denotes the material derivative,

$$\dot{f} = \frac{\partial f}{\partial t} + \boldsymbol{v} \cdot \operatorname{grad} f, \tag{2.4}$$

https://doi.org/10.1017/jfm.2018.291 Published online by Cambridge University Press

and 'grad' and 'div' denote the gradient and divergence operators. It is known that in addition to the above equations, the local form of the entropy inequality,

$$\gamma_v = \rho\,\dot{\eta} + \operatorname{div}\boldsymbol{h} \geqslant 0, \tag{2.5}$$

must be satisfied. In the above equations, $\rho > 0$ is the mass density, $\boldsymbol{v}$ the velocity, e the internal energy density, η the entropy density, γ_v the entropy production density, $\Phi = \boldsymbol{D} : \boldsymbol{\sigma}$ the mechanical energy (or stress power) with $\boldsymbol{D} = \operatorname{sym}(\operatorname{grad}\boldsymbol{v})$ ('sym' denotes the symmetric part), $\boldsymbol{\sigma}$ is the symmetric Cauchy stress tensor (the symmetry requirement arises from the balance of angular momentum), $\boldsymbol{q}$ the heat flux and $\boldsymbol{h}$ the entropy flux.

3. Constitutive equations

We note that the entropy inequality (2.5), using the energy conservation (2.3), can be rewritten in terms of the Helmholtz free energy density $\psi = e - \theta\,\eta$:

$$\gamma_v\,\theta = -\rho(\dot{\psi} + \eta\,\dot{\theta}) + \boldsymbol{D} : \boldsymbol{\sigma} - \frac{\boldsymbol{q}}{\theta}\cdot\boldsymbol{g} + \theta\operatorname{div}\boldsymbol{k} \geqslant 0, \tag{3.1}$$

where $\boldsymbol{g} \equiv \operatorname{grad}\theta$ and

$$\boldsymbol{k} \equiv \boldsymbol{h} - \frac{\boldsymbol{q}}{\theta} \tag{3.2}$$

is the extra entropy flux. We take the constitutive quantities to be given by

$$\mathcal{C} = \{\psi, \eta, \boldsymbol{q}, \boldsymbol{k}, \boldsymbol{\sigma}\} \tag{3.3}$$

and which, utilizing frame invariance, for a fluid are functions of the independent basic fields

$$\mathcal{I} = \{\rho, \boldsymbol{r}, \boldsymbol{D}, \theta, \boldsymbol{g}\}, \tag{3.4}$$

where $\theta > 0$ is the absolute temperature and $\boldsymbol{r} \equiv \operatorname{grad}\rho$. This material corresponds to a non-simple (isotropic) fluid.

Using (3.1), it can be subsequently shown that (see appendix A)

$$\psi = \psi(\rho, \theta), \tag{3.5}$$

$$\eta = -\frac{\partial\psi}{\partial\theta}, \tag{3.6}$$

and $\boldsymbol{k} = \boldsymbol{0}$, or

$$\boldsymbol{h} = \frac{\boldsymbol{q}}{\theta}. \tag{3.7}$$

Furthermore, in conjunction with (2.2) and (2.3), and the thermodynamic static equilibrium stability conditions (where $\gamma_v = 0$ when $\boldsymbol{r} = \boldsymbol{0}$, $\boldsymbol{g} = \boldsymbol{0}$, and $\boldsymbol{D} = \boldsymbol{0}$; we assume that the constitutive quantities in (3.3) have continuous second derivatives with respect to the independent basic fields in (3.4) at equilibrium), we conclude that

$$\boldsymbol{q} = \boldsymbol{q}^d(\rho, \boldsymbol{r}, \boldsymbol{D}, \theta, \boldsymbol{g}), \tag{3.8}$$

$$\boldsymbol{\sigma} = -p\,\boldsymbol{1} + \boldsymbol{\sigma}^d(\rho, \boldsymbol{r}, \boldsymbol{D}, \theta, \boldsymbol{g}), \tag{3.9}$$

where $\boldsymbol{1}$ is the unit tensor and

$$p = \rho^2\,\frac{\partial\psi}{\partial\rho} \tag{3.10}$$

https://doi.org/10.1017/jfm.2018.291 Published online by Cambridge University Press

is the thermodynamic pressure. From the above definition of a thermodynamic equilibrium state, we note that $\boldsymbol{\sigma}^d$ and $\boldsymbol{q}^d$ must vanish when $\boldsymbol{r}$, $\boldsymbol{g}$ and $\boldsymbol{D}$ vanish. In addition, using (3.8)–(3.10), the reduced entropy inequality (A 28) becomes

$$\gamma_v\,\theta = \boldsymbol{\sigma}^d : \boldsymbol{D} - \frac{\boldsymbol{q}^d}{\theta}\cdot\boldsymbol{g} \geqslant 0. \tag{3.11}$$

This inequality shows that heat, in the presence of deformation, does not, in general, flow from higher to lower temperatures.

From Paolucci (2016, tables 5.1–5.3) (see also Eringen (1980), Zheng (1993, 1994) and Liu (2002)) we can immediately write down the representations of q_i^d and σ_{ik}^d corresponding to isotropic vector-valued and symmetric tensor-valued functions of vectors $g_i = \theta_{,i}$ and $r_i = \rho_{,i}$ and symmetric second-order tensor D_{ik}:

$$q_i^d = -(\kappa_0\,\delta_{il} + \kappa_1\,D_{il} + \kappa_2\,D_{ik}D_{kl})\theta_{,l} - (\kappa_3\,\delta_{il} + \kappa_4\,D_{il} + \kappa_5\,D_{ik}D_{kl})\rho_{,l}, \tag{3.12}$$

$$\begin{aligned}\sigma_{ik}^d = {}& \alpha_0\,\delta_{ik} + \alpha_1\,D_{ik} + \alpha_2\,D_{il}D_{lk} + \alpha_3\,\theta_{,i}\theta_{,k} + \tfrac{1}{2}\,\alpha_4\,(\theta_{,i}D_{kl} + \theta_{,k}D_{il})\theta_{,l}\\ & + \tfrac{1}{2}\,\alpha_5\,(\theta_{,i}D_{kl} + \theta_{,k}D_{il})D_{lm}\theta_{,m} + \alpha_6\,\rho_{,i}\rho_{,k} + \tfrac{1}{2}\alpha_7\,(\rho_{,i}D_{kl} + \rho_{,k}D_{il})\rho_{,l}\\ & + \tfrac{1}{2}\,\alpha_8\,(\rho_{,i}D_{kl} + \rho_{,k}D_{il})D_{lm}\rho_{,m} + \tfrac{1}{2}\,\alpha_9\,(\theta_{,i}\rho_{,k} + \rho_{,i}\theta_{,k})\\ & + \tfrac{1}{2}\,\alpha_{10}[D_{il}(\rho_{,l}\theta_{,k} - \theta_{,l}\rho_{,k}) - (\rho_{,i}\theta_{,l} - \theta_{,i}\rho_{,l})D_{kl}],\end{aligned} \tag{3.13}$$

where κ_p $(p = 0, \ldots, 5)$ and α_q $(q = 0, \ldots, 10)$ are functions of ρ, θ and the isotropic scalar invariants $\{I_1, \ldots, I_{12}\}$, where

$$I_1 = D_{ii} = D_{(1)}, \tag{3.14}$$

$$I_2 = D_{ik}D_{ki} = D_{(1)}^2 - 2D_{(2)}, \tag{3.15}$$

$$I_3 = D_{ik}D_{kl}D_{li} = D_{(1)}^3 - 3D_{(1)}D_{(2)} + 3D_{(3)}, \tag{3.16}$$

$$I_4 = \theta_{,i}\theta_{,i}, \quad I_5 = \theta_{,i}D_{ik}\theta_{,k}, \quad I_6 = \theta_{,i}D_{ik}D_{kl}\theta_{,l}, \tag{3.17a–c}$$

$$I_7 = \rho_{,i}\rho_{,i}, \quad I_8 = \rho_{,i}D_{ik}\rho_{,k}, \quad I_9 = \rho_{,i}D_{ik}D_{kl}\rho_{,l}, \tag{3.18a–c}$$

$$I_{10} = \rho_{,i}\theta_{,i}, \quad I_{11} = \rho_{,i}D_{ik}\theta_{,k}, \quad I_{12} = \rho_{,i}D_{ik}D_{kl}\theta_{,l}, \tag{3.19a–c}$$

and

$$D_{(1)} = d^{(1)} + d^{(2)} + d^{(3)}, \quad D_{(2)} = d^{(1)}d^{(2)} + d^{(2)}d^{(3)} + d^{(3)}d^{(1)}, \quad D_{(3)} = d^{(1)}d^{(2)}d^{(3)}, \tag{3.20a–c}$$

where $D_{(i)}$ and $d^{(i)}$, $i = 1, 2, 3$, are the invariants and the principal deformation rates of D_{ik}, respectively. In the representation (3.13), we require that $\alpha_0 \to 0$ as $\rho_{,i} \to 0$, $\theta_{,i} \to 0$ and $D_{ik} \to 0$, since as we approach equilibrium, we must have $\sigma_{ik}^d \to 0$.

Now, substituting the representations (3.12) and (3.13) into the reduced entropy inequality (3.11), and using the Cayley–Hamilton theorem and the definitions of the invariants (3.14)–(3.19), we obtain

$$\begin{aligned}0 \leqslant \gamma_v\,\theta = {}& \alpha_0 I_1 + \alpha_1 I_2 + \alpha_2 I_3 + \left[\frac{1}{6}\alpha_5(I_1^3 - 3I_1I_2 + 2I_3) + \frac{\kappa_0}{\theta}\right] I_4\\ & + \left[\alpha_3 - \frac{1}{2}\alpha_5(I_1^2 - I_2) + \frac{\kappa_1}{\theta}\right] I_5 + \left(\alpha_4 + \alpha_5 I_1 + \frac{\kappa_2}{\theta}\right) I_6\end{aligned}$$

https://doi.org/10.1017/jfm.2018.291 Published online by Cambridge University Press

$$+\frac{1}{6}\alpha_8(I_1^3-3I_1I_2+2I_3)I_7+\left[\alpha_6-\frac{1}{2}\alpha_8(I_1^2-I_2)\right]I_8$$
$$+(\alpha_7+\alpha_8I_1)I_9+\frac{\kappa_3}{\theta}I_{10}+\left(\alpha_9+\frac{\kappa_4}{\theta}\right)I_{11}+\frac{\kappa_5}{\theta}I_{12} \tag{3.21}$$

$$\begin{aligned}=\ &\alpha_0D_{(1)}+\alpha_1(D_{(1)}^2-2D_{(2)})+\alpha_2(D_{(1)}^3-3D_{(1)}D_{(2)}+3D_{(3)})\\&+\left(\alpha_5D_{(3)}+\frac{\kappa_0}{\theta}\right)I_4+\left(\alpha_3-\alpha_5D_{(2)}+\frac{\kappa_1}{\theta}\right)I_5+\left(\alpha_4+\alpha_5D_{(1)}+\frac{\kappa_2}{\theta}\right)I_6\\&+\alpha_8D_{(3)}I_7+(\alpha_6-\alpha_8D_{(2)})I_8+(\alpha_7+\alpha_8D_{(1)})I_9+\frac{\kappa_3}{\theta}I_{10}\\&+\left(\alpha_9+\frac{\kappa_4}{\theta}\right)I_{11}+\frac{\kappa_5}{\theta}I_{12}.\end{aligned} \tag{3.22}$$

The constitutive equations (3.12) and (3.13) are too complicated for solutions of fluid problems. Generally, polynomial approximations of various degrees (denoted by 'deg') in $\boldsymbol{D}$, $\boldsymbol{r}$, and $\boldsymbol{g}$ are used. We note that $\deg I_1=\deg D_{(1)}=1$, $\deg I_2=\deg D_{(2)}=2$, $\deg I_3=\deg D_{(3)}=3$, $\deg I_4=2$, $\deg I_5=3$, $\deg I_6=4$, $\deg I_7=2$, $\deg I_8=3$, $\deg I_9=4$, $\deg I_{10}=2$, $\deg I_{11}=3$ and $\deg I_{12}=4$. Subsequently, for q_i^d to be of order N, κ_0 and κ_3, κ_1 and κ_4 and κ_2 and κ_5, can at most be of degrees $N-1$, $N-2$ and $N-3$, respectively, while for σ_{ik}^d to be of order N, α_0, α_1, α_2, α_3, α_4, α_5, α_6, α_7, α_8, α_9 and α_{10} can at most be of degrees N, $N-1$, $N-2$, $N-2$, $N-3$, $N-4$, $N-2$, $N-3$, $N-4$, $N-2$ and $N-3$, respectively.

Second-order representations

If we write second-order expansions of (3.12) and (3.13) (i.e. we take $N=2$) in the limits $\rho_{,i}\to 0$, $\theta_{,i}\to 0$ and $D_{ik}\to 0$, we require that $\kappa_0=k_{00}+k_{01}D_{(1)}$, $\kappa_1=k_{10}$, $\kappa_2=0$, $\kappa_3=k_{30}+k_{31}D_{(1)}$, $\kappa_4=k_{40}$, $\kappa_5=0$, $\alpha_0=a_{0000}+a_{0100}D_{(1)}+a_{0200}D_{(1)}^2+a_{0010}D_{(2)}+a_{0001}I_4+a_{0002}I_7+a_{0003}I_{10}$, $\alpha_1=a_{10}+a_{11}D_{(1)}$, $\alpha_2=a_{20}$, $\alpha_3=a_{30}$, $\alpha_4=\alpha_5=0$, $\alpha_6=a_{60}$, $\alpha_7=\alpha_8=0$, $\alpha_9=a_{90}$ and $\alpha_{10}=0$. Note that now k_{00}, k_{01}, k_{10}, k_{30}, k_{31}, k_{40}, a_{0000}, a_{0100}, a_{0200}, a_{0010}, a_{0001}, a_{0002}, a_{0003}, a_{10}, a_{11}, a_{20}, a_{30} and a_{60} are only functions of ρ and θ. Subsequently, since q_i^d and D_{ik}^d must vanish as $\rho_{,i}\to 0$, $\theta_{,i}\to 0$, and $D_{ik}\to 0$, we have that $a_{0000}=0$ and thus

$$q_i^d=-[(k_{00}+k_{01}D_{(1)})\delta_{il}+k_{10}D_{il}]\theta_{,l}-[(k_{30}+k_{31}D_{(1)})\delta_{il}+k_{40}D_{il}]\rho_{,l}, \tag{3.23}$$

$$\begin{aligned}\sigma_{ik}^d=\ &(a_{0100}D_{(1)}+a_{0200}D_{(1)}^2+a_{0010}D_{(2)}+a_{0001}I_4+a_{0002}I_7+a_{0003}I_{10})\delta_{ik}\\&+(a_{10}+a_{11}D_{(1)})D_{ik}+a_{20}D_{il}D_{lk}+a_{30}\theta_{,i}\theta_{,k}+a_{60}\rho_{,i}\rho_{,k}\\&+\tfrac{1}{2}a_{90}(\theta_{,i}\rho_{,k}+\rho_{,i}\theta_{,k}).\end{aligned} \tag{3.24}$$

Now, using the fact that

$$D'_{(2)}=-\tfrac{1}{2}\operatorname{tr}(\boldsymbol{D}'^2)=-\tfrac{1}{3}D_{(1)}^2+D_{(2)}, \tag{3.25}$$

where $D'_{(2)}$ denotes the second invariant of the deviatoric part of $\boldsymbol{D}$, $\boldsymbol{D}'=\boldsymbol{D}-1/3\,D_{(1)}\boldsymbol{1}$ and 'tr' denotes the trace, the residual entropy inequality (3.22) for this order of approximation becomes

$$\begin{aligned}\gamma_v\theta=\ &\left(a_{0100}+\frac{1}{3}a_{10}\right)D_{(1)}^2-2\,a_{10}D'_{(2)}+\left(a_{0200}+\frac{1}{3}a_{11}+\frac{1}{3}a_{0010}\right)D_{(1)}^3\\&+(a_{0010}-2\,a_{11}-3\,a_{20})D_{(1)}D'_{(2)}+3\,a_{20}D_{(3)}\end{aligned}$$

https://doi.org/10.1017/jfm.2018.291 Published online by Cambridge University Press

$$+\left[\frac{k_{00}}{\theta}+\left(a_{0001}+\frac{k_{01}}{\theta}\right)D_{(1)}\right]I_4+\left(a_{30}+\frac{k_{10}}{\theta}\right)I_5+a_{0002}D_{(1)}I_7$$
$$+a_{60}I_8+\left[\frac{k_{30}}{\theta}+\left(a_{0003}+\frac{k_{31}}{\theta}\right)D_{(1)}\right]I_{10}+\left(a_{90}+\frac{k_{40}}{\theta}\right)I_{11}\geqslant 0. \quad (3.26)$$

We now examine the restrictions imposed by the reduced entropy inequality (3.26) on the coefficients in (3.23) and (3.24). The inequality must be satisfied for any D_{ik} and any $\rho_{,i}$ and $\theta_{,i}$. Specifically, it must be satisfied for any of the following cases.

(1) Consider the case of a stagnant layer of fluid. In this case $\boldsymbol{D}=\boldsymbol{0}$, and the reduced entropy inequality (3.26) becomes

$$\frac{k_{00}}{\theta}I_4+\frac{k_{30}}{\theta}I_{10}\geqslant 0. \quad (3.27)$$

Since $I_4\geqslant 0$ and I_{10} can be of either sign depending on the signs of the density and temperature gradients, for the inequality to be always satisfied we must have that

$$k_{00}\geqslant 0 \quad \text{and} \quad k_{30}=0. \quad (3.28a,b)$$

(2) Subsequently, considering compressible non-isothermal motion and using the above results, the reduced entropy inequality (3.26) becomes

$$\begin{aligned}\gamma_v\theta \;=\; &\left(a_{0100}+\frac{1}{3}a_{10}\right)D_{(1)}^2-2\,a_{10}D'_{(2)}+\left(a_{0200}+\frac{1}{3}a_{11}+\frac{1}{3}a_{0010}\right)D_{(1)}^3\\&+(a_{0010}-2\,a_{11}-3\,a_{20})D_{(1)}D'_{(2)}+3\,a_{20}D_{(3)}\\&+\left[\frac{k_{00}}{\theta}+\left(a_{0001}+\frac{k_{01}}{\theta}\right)D_{(1)}\right]I_4+\left(a_{30}+\frac{k_{10}}{\theta}\right)I_5+a_{0002}D_{(1)}I_7\\&+a_{60}I_8+\left(a_{0003}+\frac{k_{31}}{\theta}\right)D_{(1)}I_{10}+\left(a_{90}+\frac{k_{40}}{\theta}\right)I_{11}\geqslant 0.\end{aligned} \quad (3.29)$$

Since $D'_{(2)}\leqslant 0$, it is now easy to see that for the inequality to be satisfied for arbitrary motions, we must have that

$$\left.\begin{gathered}a_{0100}+\tfrac{1}{3}a_{10}\geqslant 0,\quad a_{10}\geqslant 0,\quad a_{0200}+\tfrac{1}{3}a_{11}+\tfrac{1}{3}a_{0010}=0,\\ a_{0010}-2\,a_{11}-3\,a_{20}=0,\\ a_{20}=0,\quad a_{0001}+\frac{k_{01}}{\theta}=0,\quad a_{30}+\frac{k_{10}}{\theta}=0,\quad a_{0002}=0,\quad a_{60}=0,\\ a_{0003}+\frac{k_{31}}{\theta}=0,\quad a_{90}+\frac{k_{40}}{\theta}=0.\end{gathered}\right\} \quad (3.30)$$

In summary, we have that

$$\left.\begin{gathered}k_{00}\geqslant 0,\quad a_{0100}+\tfrac{1}{3}a_{10}\geqslant 0,\quad a_{10}\geqslant 0,\quad a_{0010}=2\,a_{11},\quad a_{0200}=-a_{11},\\ a_{0001}=-\frac{k_{01}}{\theta},\quad a_{30}=-\frac{k_{10}}{\theta},\quad a_{0003}=-\frac{k_{31}}{\theta},\quad a_{90}=-\frac{k_{40}}{\theta},\\ k_{30}=a_{0002}=a_{20}=a_{60}=0,\end{gathered}\right\} \quad (3.31)$$

https://doi.org/10.1017/jfm.2018.291 Published online by Cambridge University Press

and k_{01}, k_{10}, k_{31} and k_{40} can be of any sign. If we rewrite the above by taking $a_{0100} = \lambda$, $a_{10} = 2\,\mu$, $a_{11} = \mu'$, $k_{00} = k$, $k_{01} = k'$, $k_{10} = k''$, $k_{31} = k'''$ and $k_{40} = k''''$, then the quadratic constitutive representations (3.23) and (3.24) for $\boldsymbol{q}^d$ and $\boldsymbol{\sigma}^d$ become

$$q_i = -[(k + k' D_{(1)})\delta_{il} + k'' D_{il}]\theta_{,l} - (k''' D_{(1)}\delta_{il} + k'''' D_{il})\rho_{,l}, \tag{3.32}$$

$$\sigma_{ik} = \left(-p + \lambda D_{(1)} - \mu' D_{jl} D_{lj} - \frac{k'}{\theta}\,\theta_{,j}\theta_{,j} - \frac{k'''}{\theta}\,\rho_{,j}\theta_{,j}\right)\delta_{ik} + (2\,\mu + \mu' D_{(1)}) D_{ik} - \frac{k''}{\theta}\,\theta_{,i}\theta_{,k} - \frac{1}{2}\frac{k''''}{\theta}(\theta_{,i}\rho_{,k} + \rho_{,i}\theta_{,k}), \tag{3.33}$$

and the reduced entropy inequality (3.26), rewritten as

$$\gamma_v\,\theta = \zeta\, D_{(1)}^2 - 4\,\mu\, D'_{(2)} + \frac{k}{\theta}\, I_4 \geqslant 0, \tag{3.34}$$

is always satisfied when

$$\mu \geqslant 0, \quad \kappa \equiv \lambda + \tfrac{2}{3}\,\mu \geqslant 0, \quad k \geqslant 0 \quad \text{and} \quad \{\mu', k', k'', k''', k''''\} \in \mathrm{R}, \tag{3.35a–d}$$

where κ, λ, μ and μ' are respectively the bulk viscosity, the dilatational viscosity, the shear viscosity and a second shear viscosity, and k, k', k'', k''' and k'''' are the standard and higher thermal conductivities. All such properties are functions of the density, ρ, and temperature, θ.

The first three restrictions in (3.35) are the same restrictions obtained from the linear theory. Note that in the linear theory (3.32) and (3.33) reduce to the classical Fourier and Navier–Cauchy–Poisson constitutive equations, respectively.

The additional viscous property, μ', and the four additional thermal properties, k', k'', k''' and k'''', can be of any sign and do not contribute to entropy production. However, they do contribute to the mechanical pressure,

$$\overline{p} \equiv -\tfrac{1}{3}\sigma_{kk}, \tag{3.36}$$

since

$$-\overline{p} = -p + \kappa\, D_{(1)} - \frac{2}{3}\,\mu' D_{(1)}^2 + 2\,\mu' D_{(2)} - \frac{\left(k' + \frac{1}{3}\,k''\right)}{\theta}\,\theta_{,i}\theta_{,i} - \frac{\left(k''' + \frac{1}{3}\,k''''\right)}{\theta}\,\rho_{,i}\theta_{,i}, \tag{3.37}$$

and in this case, the mechanical pressure is not equal to the thermodynamic pressure even when the fluid is incompressible (i.e. when $D_{(1)} = 0$). Furthermore, while in the classical linear theory, we have that $p \geqslant \overline{p}$ in an expansion and $p \leqslant \overline{p}$ in a contraction motion, the above equation shows that the sign of $(p - \overline{p})$ does not necessarily follow the intuitive notion of being positive on expansion and negative on contraction motion.

3.1. *Equations of state*

To close the problem, we require a fundamental thermodynamic relation for the fluid; we shall write this in terms of the Helmholtz free energy $\psi = \psi(\rho, \theta)$. From this relation, the pressure, internal energy, enthalpy and density (p, e, h and ρ) are given by the thermal and caloric equations of state:

$$e = e(\rho, \theta) = \psi - \theta\,\frac{\partial \psi}{\partial \theta} \quad \text{or} \quad h = h(\rho, \theta) = \psi - \theta\,\frac{\partial \psi}{\partial \theta} + \rho\,\frac{\partial \psi}{\partial \rho}, \tag{3.38a,b}$$

$$p = p(\rho, \theta) = \rho^2\,\frac{\partial \psi}{\partial \rho}. \tag{3.39}$$

https://doi.org/10.1017/jfm.2018.291 Published online by Cambridge University Press

In general, we can show that for any isotropic material

$$\mathrm{d}p = \frac{1}{\kappa_\theta}\left(\frac{1}{\rho}\,\mathrm{d}\rho + \alpha\,\mathrm{d}\theta\right) \tag{3.40}$$

and

$$\rho\,\mathrm{d}e = \frac{1}{\rho}\left(p - \frac{\alpha}{\kappa_\theta}\,\theta\right)\mathrm{d}\rho + \rho\,c_v\,\mathrm{d}\theta \tag{3.41}$$

or

$$\rho\,\mathrm{d}h = \frac{1}{\rho\,\kappa_\theta}(1-\alpha\,\theta)\,\mathrm{d}\rho + \left(\rho\,c_v + \frac{\alpha}{\kappa_\theta}\right)\mathrm{d}\theta, \tag{3.42}$$

where

$$c_v \equiv \left.\frac{\partial e}{\partial \theta}\right|_\rho, \quad c_p \equiv \left.\frac{\partial h}{\partial \theta}\right|_p, \quad \kappa_\theta \equiv \frac{1}{\rho}\left.\frac{\partial \rho}{\partial p}\right|_\theta \quad \text{and} \quad \alpha \equiv -\frac{1}{\rho}\left.\frac{\partial \rho}{\partial \theta}\right|_p \tag{3.43a–d}$$

are the coefficients of specific heat at constant volume, specific heat at constant pressure, isothermal compressibility and volume expansion, respectively. From equilibrium thermodynamics stability considerations, we have the following additional restrictions (see Paolucci 2016):

$$c_v > 0, \quad \gamma \equiv \frac{c_p}{c_v} > 1, \quad \kappa_\theta > 0 \quad \text{and} \quad \alpha^2 < \frac{\rho\,c_p\,\kappa_\theta}{\theta}. \tag{3.44a–d}$$

These are well-known results since the dependence of ψ on ρ and θ is the same as in the classical NSF theory.

In the present work we use the free energy of a perfect gas with constant specific heats

$$\psi(\rho,\theta) = R\,\theta\,\ln\rho + f(\theta) = e_0 - \theta\,\eta_0 + \theta[c_v\,(1-\ln\,\theta) + R\,\ln\,\rho], \tag{3.45}$$

where e_0 and η_0 are constants, and c_v and $R = c_p - c_v$ are positive constants. In this case we have that

$$\eta(\rho,\theta) = -\left.\frac{\partial \psi}{\partial \theta}\right|_\rho = -R\,\ln\rho + f'(\theta) = \eta_0 + c_v\,\ln\,\theta - R\,\ln\,\rho, \tag{3.46}$$

and it is easy to see that the thermal and caloric equations of state are

$$p(\rho,\theta) = R\,\rho\,\theta \tag{3.47}$$

and

$$e(\rho,\theta) = \psi(\rho,\theta) + \eta(\rho,\theta)\,\theta = f(\theta) - \theta f'(\theta) = e(\theta) = c_v\,\theta \tag{3.48}$$

or

$$h(\rho,\theta) = e(\rho,\theta) + \frac{p(\rho,\theta)}{\rho} = h(\theta) = c_p\,\theta. \tag{3.49}$$

https://doi.org/10.1017/jfm.2018.291 Published online by Cambridge University Press

4. The one-dimensional shock structure

For one-dimensional flow, the equations for conservation of mass, linear momentum and energy (2.1)–(2.3) become

$$\frac{\partial \rho}{\partial t} + \frac{\partial}{\partial x}(\rho\, u) = 0, \tag{4.1}$$

$$\frac{\partial}{\partial t}(\rho\, u) + \frac{\partial}{\partial x}(\rho\, u^2 - \sigma_{11}) = 0, \tag{4.2}$$

$$\frac{\partial}{\partial t}\left[\rho\left(e + \frac{1}{2}u^2\right)\right] + \frac{\partial}{\partial x}\left[\rho\left(e + \frac{1}{2}u^2\right) u - \sigma_{11} u + q_1\right] = 0. \tag{4.3}$$

The heat flux and Cauchy stress tensor (3.32) and (3.33) in one dimension are given by

$$q_1 = -[(k + k'\, D_{(1)})\delta_{11} + k''\, D_{11}]\theta_{,1} - (k'''\, D_{(1)}\delta_{11} + k''''\, D_{11})\rho_{,1}, \tag{4.4}$$

$$\sigma_{11} = \left(-p + \lambda\, D_{(1)} - \mu'\, D_{11}\, D_{11} - \frac{k'}{\theta}\,\theta_{,1}\,\theta_{,1} - \frac{k'''}{\theta}\,\rho_{,1}\,\theta_{,1}\right)\delta_{11} + (2\,\mu + \mu'\, D_{(1)})D_{11} - \frac{k''}{\theta}\,\theta_{,1}\,\theta_{,1} - \frac{k''''}{\theta}\,\rho_{,1}\,\theta_{,1}. \tag{4.5}$$

Furthermore, δ_{11}, $D_{11} = \partial u/\partial x$ and $D_{(1)} = \operatorname{tr} \boldsymbol{D} = \partial u/\partial x$ are the '11'-component of the Kronecker delta, and the '11'-component and first invariant of the stretch tensor D_{ik} in one dimension.

Subsequently, the heat flux and the Cauchy stress tensor simplify to the following equations:

$$q_1 = -\left(k + k^{\star}\,\frac{\partial u}{\partial x}\right)\frac{\partial \theta}{\partial x} - k^{\star\star}\frac{\partial u}{\partial x}\,\frac{\partial \rho}{\partial x}, \tag{4.6}$$

$$\sigma_{11} = -p + \tau_{11} = -p + \zeta\,\frac{\partial u}{\partial x} - \frac{k^{\star}}{\theta}\left(\frac{\partial \theta}{\partial x}\right)^2 - \frac{k^{\star\star}}{\theta}\,\frac{\partial \rho}{\partial x}\,\frac{\partial \theta}{\partial x}, \tag{4.7}$$

where τ_{11} is the '11'-component of the shear stress tensor,

$$\zeta \equiv \tfrac{4}{3}\,\mu + \kappa, \quad k^{\star} = k' + k'' \quad \text{and} \quad k^{\star\star} = k''' + k''''. \tag{4.8}$$

Note that in one dimension the terms involving the second shear viscosity, μ', cancel! Furthermore, the higher thermal conductivities combine into two quantities.

4.1. *Reduced system*

If we take the shock to move at constant velocity U and locate the origin of the coordinate system X on the shock, i.e. we take

$$X = x - U\, t, \tag{4.9}$$

then we can write

$$\frac{\partial}{\partial t} = -U\,\frac{\mathrm{d}}{\mathrm{d}X} \quad \text{and} \quad \frac{\partial}{\partial x} = \frac{\mathrm{d}}{\mathrm{d}X}. \tag{4.10a,b}$$

https://doi.org/10.1017/jfm.2018.291 Published online by Cambridge University Press

Subsequently, equations (4.1)–(4.3) can be rewritten as

$$-U\frac{\mathrm{d}\rho}{\mathrm{d}X}+\frac{\mathrm{d}}{\mathrm{d}X}(\rho u)=0, \tag{4.11}$$

$$-U\frac{\mathrm{d}}{\mathrm{d}X}(\rho u)+\frac{\mathrm{d}}{\mathrm{d}X}(\rho u^2-\sigma_{11})=0, \tag{4.12}$$

$$-U\frac{\mathrm{d}}{\mathrm{d}X}\left[\rho\left(e+\tfrac{1}{2}u^2\right)\right]+\frac{\mathrm{d}}{\mathrm{d}X}\left[\rho\left(e+\frac{1}{2}u^2\right)u-\sigma_{11}u+q_1\right]=0. \tag{4.13}$$

If we integrate the equations, evaluate the constants of integration by taking $X\to-\infty$ where $\tau_{11}=0$ and $q_1=0$, where we denote conditions at that limit by the subscript '1', and take

$$v=u-U, \tag{4.14}$$

then the integrals of the above equations can be rewritten in the following forms:

$$\rho v=\rho_1 v_1, \tag{4.15}$$

$$\rho v^2+p-\tau_{11}=\rho_1 v_1^2+p_1, \tag{4.16}$$

$$\rho\left(e+\tfrac{1}{2}v^2\right)v+pv-\tau_{11}v+q_1=\rho_1\left(e_1+\tfrac{1}{2}v_1^2\right)v_1+p_1v_1, \tag{4.17}$$

and since $h=e+p/\rho$, we can alternatively write the energy equation (4.17) in the form

$$\rho v\left(h+\tfrac{1}{2}v^2\right)-\tau_{11}v+q_1=\rho_1 v_1\left(h_1+\tfrac{1}{2}v_1^2\right). \tag{4.18}$$

Equations (4.15), (4.16) and (4.18) can be simplified and solved for τ_{11} and q_1:

$$\tau_{11}=\rho_1 v_1(v-v_1)+(p-p_1), \tag{4.19}$$

$$q_1=-\rho_1 v_1\left[(h-h_1)-\tfrac{1}{2}(v-v_1)^2\right]+(p-p_1)v. \tag{4.20}$$

The right-hand sides yield the Rankine–Hugoniot conditions relating the quantities since as $X\to\pm\infty$, $\tau_{11}\to 0$ and $q_1\to 0$. These will provide the boundary conditions to the reduced system (see below).

4.2. *Dimensionless system*

To make the problem dimensionless, we introduce reference quantities based upon the upstream conditions:

$$X=\lambda_1 X',\quad v=c_1 v',\quad \rho=\rho_1\rho',\quad p=(\rho_1 c_1^2)p',\quad \theta=\theta_1\theta',\quad h=h_1 h', \tag{4.21a–f}$$

$$\zeta=\mu_1\zeta',\quad k=k_1 k',\quad k^{\star}=\left(\frac{\mu^2}{\rho\theta}\right)k^{\star\prime},\quad k^{\star\star}=\left(\frac{\mu}{\rho}\right)^2 k^{\star\star\prime}, \tag{4.22a–d}$$

where we have

$$\lambda_1=\delta\frac{\mu_1}{\rho_1 c_1},\quad c_1=\sqrt{\frac{\gamma p_1}{\rho_1}}=\sqrt{\gamma R\theta_1},\quad h_1=c_p\theta_1,\quad \gamma=\frac{c_p}{c_v},\quad R=c_p-c_v, \tag{4.23a–e}$$

and note that λ_1 is the Maxwellian mean free path with constant

$$\delta\equiv\frac{16}{5}\sqrt{\frac{\gamma}{2\pi}}, \tag{4.24}$$

https://doi.org/10.1017/jfm.2018.291 Published online by Cambridge University Press

and c_1 is the sound speed. The scalings used for the new properties in (4.22) reflect the Truesdell dimensional invariance principle (see Truesdell & Noll 2004). The resulting scaled constitutive equations are of the same form as obtained by the Chapman–Enskog process in kinetic theory, where these dimensionless properties are given as constant values (see § 6). In our case, the dimensionless properties are now functions of the dimensionless density and temperature.

Now, substituting (4.21) and (4.22) into (4.19) and (4.20) using the constitutive equations (4.6) and (4.7) (with (4.10), (4.14) and (4.23)), recognizing the dimensionless mass balance corresponding to (4.15),

$$\rho' v' = M_1, \tag{4.25}$$

and dimensionless equations of state corresponding to (3.47) and (3.49),

$$p' = \frac{1}{\gamma}\rho'\theta' \quad \text{and} \quad h' = \theta', \tag{4.26a,b}$$

and subsequently dropping the primes, we obtain the following system of ordinary differential equations (ODEs) for the dimensionless velocity and temperature:

$$\boldsymbol{A}\cdot\frac{\mathrm{d}\boldsymbol{f}}{\mathrm{d}X} = (\delta M_1)^2\boldsymbol{F}, \tag{4.27}$$

where $\boldsymbol{f} = (v\ \ \theta)^{\mathrm{T}}$,

$$\boldsymbol{A} = \begin{pmatrix} \delta M_1\,\zeta\,\theta & -\left(k^\star\dfrac{v}{\theta}\dfrac{\mathrm{d}\theta}{\mathrm{d}X} - k^{\star\star}\dfrac{\mathrm{d}v}{\mathrm{d}X}\right) \\ -\left(k^\star\dfrac{v}{\theta}\dfrac{\mathrm{d}\theta}{\mathrm{d}X} - k^{\star\star}\dfrac{\mathrm{d}v}{\mathrm{d}X}\right) & \dfrac{\delta M_1}{(\gamma-1)\,Pr}\,k \end{pmatrix}, \tag{4.28}$$

$$\boldsymbol{F} = \begin{pmatrix} \theta\left[(v-M_1) + \dfrac{1}{\gamma}\left(\dfrac{\theta}{v} - \dfrac{1}{M_1}\right)\right] \\ \left[\dfrac{1}{\gamma-1}(\theta-1) - \dfrac{1}{\gamma}\left(\theta - \dfrac{v}{M_1}\right) - \dfrac{1}{2}(v-M_1)^2\right] \end{pmatrix}, \tag{4.29}$$

and we have the dimensionless parameters

$$M_1 = \frac{v_1}{c_1}, \quad Pr = \frac{\mu_1 c_p}{k_1}, \quad \gamma = \frac{c_p}{c_v}. \tag{4.30a–c}$$

We note that A is symmetric,

$$\det\boldsymbol{A} = \frac{(\delta M_1)^2}{(\gamma-1)\,Pr}\,\zeta\,k\,\theta - \left(k^\star\frac{v}{\theta}\frac{\mathrm{d}\theta}{\mathrm{d}X} - k^{\star\star}\frac{\mathrm{d}v}{\mathrm{d}X}\right)^2, \tag{4.31}$$

and it is zero when $\zeta = 0$ or $k = 0$, and $k^\star = k^{\star\star} = 0$. Furthermore,

$$\boldsymbol{A}^{-1} = \frac{1}{\det\boldsymbol{A}}\begin{pmatrix} \dfrac{\delta M_1}{(\gamma-1)\,Pr}\,k & \left(k^\star\dfrac{v}{\theta}\dfrac{\mathrm{d}\theta}{\mathrm{d}X} - k^{\star\star}\dfrac{\mathrm{d}v}{\mathrm{d}X}\right) \\ \left(k^\star\dfrac{v}{\theta}\dfrac{\mathrm{d}\theta}{\mathrm{d}X} - k^{\star\star}\dfrac{\mathrm{d}v}{\mathrm{d}X}\right) & \delta M_1\,\zeta\,\theta \end{pmatrix}. \tag{4.32}$$

https://doi.org/10.1017/jfm.2018.291 Published online by Cambridge University Press

Subsequently, the system (4.27) can be written in the form

$$\frac{\mathrm{d}\boldsymbol{f}}{\mathrm{d}X} = (\delta M_1)^2 \frac{\boldsymbol{G}}{\det \boldsymbol{A}}, \tag{4.33}$$

where

$$\boldsymbol{G} = \begin{pmatrix} \dfrac{\delta M_1}{(\gamma-1)Pr}\, k F_1 + \left(k^\star \dfrac{v}{\theta}\dfrac{\mathrm{d}\theta}{\mathrm{d}X} - k^{\star\star}\dfrac{\mathrm{d}v}{\mathrm{d}X}\right) F_2, \\ \left(k^\star \dfrac{v}{\theta}\dfrac{\mathrm{d}\theta}{\mathrm{d}X} - k^{\star\star}\dfrac{\mathrm{d}v}{\mathrm{d}X}\right) F_1 + \delta M_1\, \zeta\, \theta\, F_2 \end{pmatrix}. \tag{4.34}$$

The boundary conditions are given by

$$\boldsymbol{f}(-\infty) \to \boldsymbol{f}_1 = \begin{pmatrix} M_1 \\ 1 \end{pmatrix} \quad \text{and} \quad \boldsymbol{f}(+\infty) \to \boldsymbol{f}_2 = \begin{pmatrix} M_1 \dfrac{v_2}{v_1} \\ \dfrac{\theta_2}{\theta_1} \end{pmatrix}. \tag{4.35a,b}$$

Note that all kinetic theories applied to this problem obtain a system which for $(v\ \ \theta)^{\mathrm{T}}$ look like (4.27), but in all cases the corresponding matrix $\boldsymbol{A}$ (see (4.28)) becomes singular at some Mach number. In our case, it is never singular (see (4.31)).

4.3. *Rankine–Hugoniot relations*

From the equilibrium conditions at $X \to \pm\infty$, it is straightforward to use the balance equations to obtain the Rankine–Hugoniot relations. These are relations for the unknown quantities at $X \to +\infty$ (using subscripts '2') in terms of known quantities at $X \to -\infty$ (using subscripts '1'). Among those, we list below the ones relevant to us:

$$\frac{v_2}{v_1} = \frac{2+(\gamma-1)M_1^2}{(\gamma+1)M_1^2}, \tag{4.36}$$

$$\frac{\theta_2}{\theta_1} = 1 + \frac{2(\gamma-1)}{(\gamma+1)^2}\,\frac{\gamma M_1^2+1}{M_1^2}\,(M_1^2-1), \tag{4.37}$$

$$M_2^2 = \frac{2+(\gamma-1)M_1^2}{2\gamma M_1^2-(\gamma-1)}. \tag{4.38}$$

Subsequently, the boundary conditions (4.35*a*,*b*) become

$$\boldsymbol{f}(-\infty) \to \boldsymbol{f}_1 = \begin{pmatrix} M_1 \\ 1 \end{pmatrix} \tag{4.39}$$

and

$$\boldsymbol{f}(+\infty) \to \boldsymbol{f}_2 = \begin{pmatrix} \dfrac{2+(\gamma-1)M_1^2}{(\gamma+1)M_1} \\ 1 + \dfrac{2(\gamma-1)}{(\gamma+1)^2}\,\dfrac{\gamma M_1^2+1}{M_1^2}\,(M_1^2-1) \end{pmatrix}. \tag{4.40}$$

https://doi.org/10.1017/jfm.2018.291 Published online by Cambridge University Press

5. Results

Studies of shock structure are generally validated by comparing the reciprocal density thickness, λ_1/L, with experimental measurements, where the thickness is conventionally defined as

$$L = (\rho_2 - \rho_1) \Big/ \left. \frac{\mathrm{d}\rho}{\mathrm{d}x} \right|_{max}. \tag{5.1}$$

We have kept the usual maximum slope definition of the shock thickness to make comparisons with previous works.

Another quantity that is sometimes used for validation is the asymmetry of the density profiles, defined as

$$Q = \int_{-\infty}^{0} \rho_n \, \mathrm{d}x \Big/ \int_{0}^{\infty} (1 - \rho_n) \, \mathrm{d}x. \tag{5.2}$$

Much more critical validation is provided by comparing the actual density distributions within the shock for varying upstream Mach numbers with accurate experimental measurements of Alsmeyer (1976) for argon and nitrogen gases.

To compute the shock structure, we have to specify the dependence of the transport properties on density and temperature. To maintain some degree of generality, we assume that all transport properties are of power law forms:

$$\left.\begin{aligned} \mu = \mu(\rho,\theta) = \rho^{\beta_1}\theta^{\gamma_1}, \quad \kappa = \kappa(\rho,\theta) = \kappa_0\rho^{\beta_2}\theta^{\gamma_2}, \quad k = k(\rho,\theta) = \rho^{\beta_3}\theta^{\gamma_3}, \\ k^\star = k^\star(\rho,\theta) = k_0^\star\rho^{\beta_4}\theta^{\gamma_4}, \quad k^{\star\star} = k^{\star\star}(\rho,\theta) = k_0^{\star\star}\rho^{\beta_5}\theta^{\gamma_5}, \end{aligned}\right\} \tag{5.3}$$

where the β_i values and γ_i values are free parameters. Given that experimental information on such properties is not available at all or for the conditions encountered within the shock structure at varying Mach numbers, we will select the parameters appearing in (5.3) by comparing the computed solutions to those measured by Alsmeyer (1976). All constants have been selected to yield good quantitative agreements to the shock reciprocal thickness and asymmetry of the experimental density distributions at four different Mach numbers. Note that the values of the constants have not been optimized to yield the minimum differences between the computed results and the experimental values. The parameter values obtained for argon and nitrogen gases are as follows.

Argon: $\beta_1 = 0.5$, $\gamma_1 = 0.72$, $\kappa_0 = 0$, $\beta_2 = 0$, $\gamma_2 = 0$, $\beta_3 = 0.5$, $\gamma_3 = 0.73$, $k_0^\star = 1.0$, $\beta_4 = \gamma_4 = 0.5$, $k_0^{\star\star} = 4.0$, $\beta_4 = \gamma_4 = 0.5$.

Nitrogen: $\beta_1 = \gamma_1 = 0.67$, $\kappa_0 = 0.4$, $\beta_2 = 0.0$, $\gamma_2 = 1.0$, $\beta_3 = \gamma_3 = 0.74$, $k_0^\star = 2.0$, $\beta_4 = 0.5$, $\gamma_4 = 0.25$, $k_0^{\star\star} = 4.0$, $\beta_4 = 0.5$, $\gamma_4 = 0.25$.

The system (4.33) with boundary conditions (4.39) and (4.40) has been solved using the MATLAB routine `ode15i` with maximum order of 5. The routine utilizes a shooting method. The integration is performed from the unstable direction of the associated saddle point in the downstream to the connecting stable direction associated with the node point in the upstream. The initial downstream point (which is an equilibrium point) is perturbed in the unstable direction and subsequently the MATLAB routine `decic` is used to adjust the perturbation so as to provide consistent initial conditions. To perform the integration, the relative and absolute errors used are 10^{-13} and 10^{-14}, respectively.

https://doi.org/10.1017/jfm.2018.291 Published online by Cambridge University Press

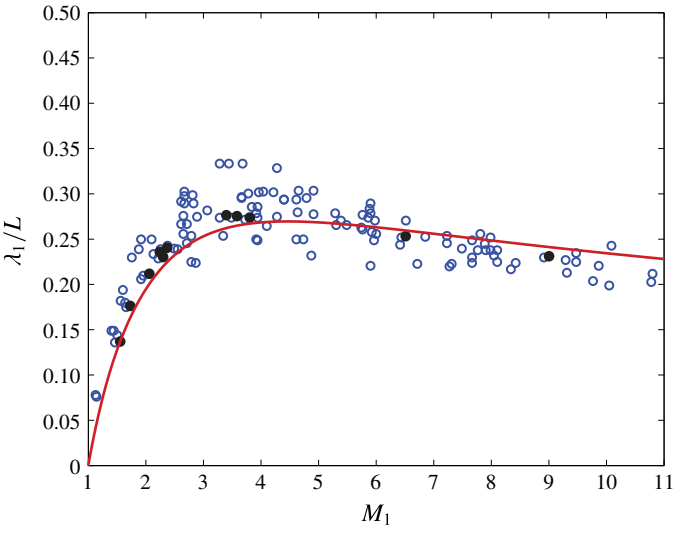


FIGURE 2. (Colour online) Inverse shock thickness, λ_1/L, as a function of upstream Mach number, M_1, in argon gas: ○, experimental results of Linzer & Hornig (1963), Camac (1965), Russell (1965), Schultz-Grunow & Frohn (1965), Robben & Talbot (1966), Schmidt (1969), Rieutord (1970) and Garen *et al.* (1974); ●, experimental results of Alsmeyer (1976); ——, present theory.

Figure 2 compares the experimentally measured inverse shock thickness and our results over a large Mach number range for argon gas (note that in this case the bulk viscosity is identically zero). Our results are in good agreement with the experimental results of Alsmeyer (1976).

In figure 3 we provide the corresponding asymmetry of the density profiles for the argon gas, over the same Mach number range. Again, our result is in reasonable agreement with the experimental data, in particular when compared to the asymmetry resulting from the NSF theory.

More critical comparisons for the argon gas are provided by comparing the actual density distributions. Such distributions for Mach numbers 1.55, 1.75, 3.8 and 9.0 are shown in figure 4. Our results are in excellent agreement with the experimental data of Alsmeyer (1976). With the exception of the DSMC results (see Alsmeyer 1976), this is not the case for the distributions obtained from the various second-order expansions of the Boltzmann equation (e.g. Reese *et al.* 1995) or from the modified Brenner equation (see Greenshields & Reese 2007).

Analogous results, and comparisons to experimental data where available, for the inverse shock thickness, asymmetry of density profiles and density distributions for the same Mach numbers for nitrogen gas (in this case the bulk viscosity is not zero) are provided in figures 5, 6 and 7, respectively. We make the following observations. First, as in the case for argon, the inverse shock thickness for nitrogen is in relatively good agreement with the experimental results. Second, to the authors' knowledge, no experimental results are available for the asymmetry of the density profiles for nitrogen, and thus we just provide the result obtained from the present second-order theory. Lastly, as observed from figure 7, for nitrogen gas we again have excellent agreement of the density profiles between our theory and experimental results.

https://doi.org/10.1017/jfm.2018.291 Published online by Cambridge University Press

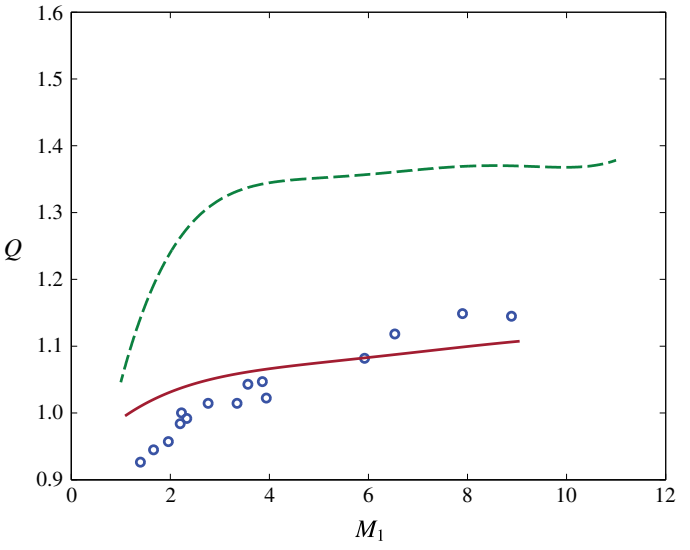


FIGURE 3. (Colour online) Asymmetry of density profiles, Q, as a function of upstream Mach number, M_1, in argon gas: ○, experimental results of Schmidt (1969) and Alsmeyer (1976); – – –, NSF theory; ——, present theory.

6. Discussion and conclusions

We next compare our second-order continuum theory obtained through an expansion in strain rate and gradients of density and temperature with the second-order theory obtained through the Chapman–Enskog expansion in Knudsen number. To facilitate this, we rewrite our constitutive equations (4.6) and (4.7) in dimensional form but with dimensionless new parameters (which are functions of dimensionless density and temperature),

$$q = -k\frac{\mathrm{d}\theta}{\mathrm{d}x} - k^{\star\prime}\frac{\mu^2}{\rho\,\theta}\frac{\mathrm{d}u}{\mathrm{d}x}\frac{\mathrm{d}\theta}{\mathrm{d}x} - k^{\star\star\prime}\left(\frac{\mu}{\rho}\right)^2\frac{\mathrm{d}\rho}{\mathrm{d}x}\frac{\mathrm{d}u}{\mathrm{d}x}, \tag{6.1}$$

$$\sigma = -p + \zeta\frac{\mathrm{d}u}{\mathrm{d}x} - k^{\star\prime}\frac{\mu^2}{\rho\,\theta^2}\left(\frac{\mathrm{d}\theta}{\mathrm{d}x}\right)^2 - k^{\star\star\prime}\frac{\mu^2}{\rho^2\theta}\frac{\mathrm{d}\rho}{\mathrm{d}x}\frac{\mathrm{d}\theta}{\mathrm{d}x}, \tag{6.2}$$

so as to write them in the same form obtained through the Chapman–Enskog expansion for a monatomic gas (see Lumpkin & Chapman 1992; Reese *et al.* 1995),

$$q = -k\frac{\mathrm{d}\theta}{\mathrm{d}x} + c_1\frac{\mu^2}{\rho\,\theta}\frac{\mathrm{d}u}{\mathrm{d}x}\frac{\mathrm{d}\theta}{\mathrm{d}x} + c_2\left(\frac{\mu}{\rho}\right)^2\frac{\mathrm{d}\rho}{\mathrm{d}x}\frac{\mathrm{d}u}{\mathrm{d}x} \underbrace{- c_3\frac{\mu^2}{\rho}\frac{\mathrm{d}^2u}{\mathrm{d}x^2}}_{(3)}, \tag{6.3}$$

$$\sigma = -p + \frac{4}{3}\mu\frac{\mathrm{d}u}{\mathrm{d}x} \underbrace{- c_4\frac{\mu^2}{p}\left(\frac{\mathrm{d}u}{\mathrm{d}x}\right)^2}_{(1)} - c_5\frac{\mu^2}{\rho\,\theta^2}\left(\frac{\mathrm{d}\theta}{\mathrm{d}x}\right)^2 + c_6\frac{\mu^2}{\rho^2\theta}\frac{\mathrm{d}\rho}{\mathrm{d}x}\frac{\mathrm{d}\theta}{\mathrm{d}x}$$

$$\underbrace{- c_7\frac{\mu^2}{\rho^3}\left(\frac{\mathrm{d}\rho}{\mathrm{d}x}\right)^2}_{(2)} \underbrace{+ c_8\frac{\mu^2}{\rho\,\theta}\frac{\mathrm{d}^2\theta}{\mathrm{d}x^2} + c_9\frac{\mu^2}{\rho^2}\frac{\mathrm{d}^2\rho}{\mathrm{d}x^2}}_{(3)}, \tag{6.4}$$

https://doi.org/10.1017/jfm.2018.291 Published online by Cambridge University Press

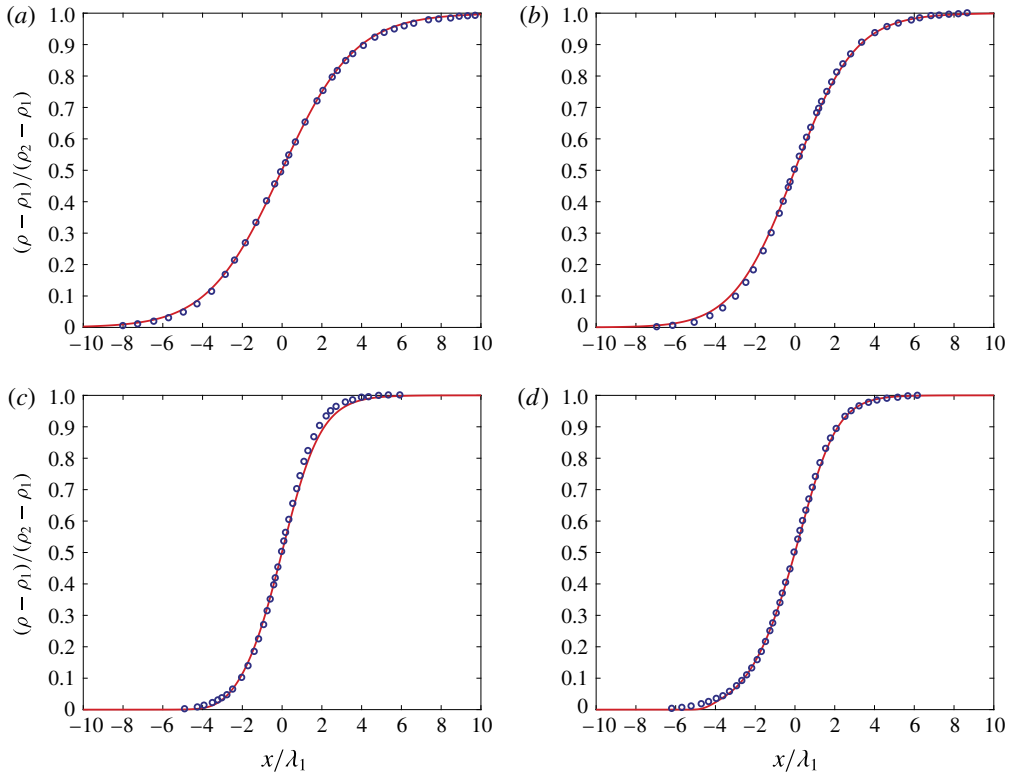


FIGURE 4. (Colour online) Shock density profiles in argon gas for (*a*) $M_1 = 1.55$, (*b*) $M_1 = 1.75$, (*c*) $M_1 = 3.8$ and (*d*) $M_1 = 9.0$: ——, present theory; ○, experimental results of Alsmeyer (1976).

where all c_i values are dimensionless constants obtained from collision integrals. We have identified several terms in the latter equations to facilitate the following discussion. In comparing the constitutive equations, we first note that for a monatomic gas $\kappa = 0$ so that $\zeta = 4/3\,\mu$. Subsequently, all terms in our constitutive equations (6.1) and (6.2) are also present in the corresponding equations (6.3) and (6.4). But, the constitutive equations obtained from kinetic theory have additional terms that we discuss below.

Term (1), which is quadratic in the velocity gradient, does not appear in (6.2) since the two terms that are quadratic in the velocity gradient in (4.5) cancel in the one-dimensional problem of the shock structure. This would suggest that c_4 in (6.4) should be zero; Lumpkin & Chapman (1992) (see also Reese *et al.* 1995) report $c_4 = -12.31$.

Term (2), which is quadratic in the density gradient, does not appear in (6.2). While such terms do appear in the general second-order representation (3.24) (see the terms multiplied by a_{0002} and a_{60}), the reduced entropy inequality (3.26) requires that $a_{0002} = a_{60} = 0$. This would suggest that c_7 should be zero; Lumpkin and Chapman report $c_7 = 1.75$. Our conclusion regarding this term is consistent with the results of Comeaux *et al.* (1995) who showed that the Burnett equations can violate the second law of thermodynamics and this may be the cause for the instability encountered in their solution.

https://doi.org/10.1017/jfm.2018.291 Published online by Cambridge University Press

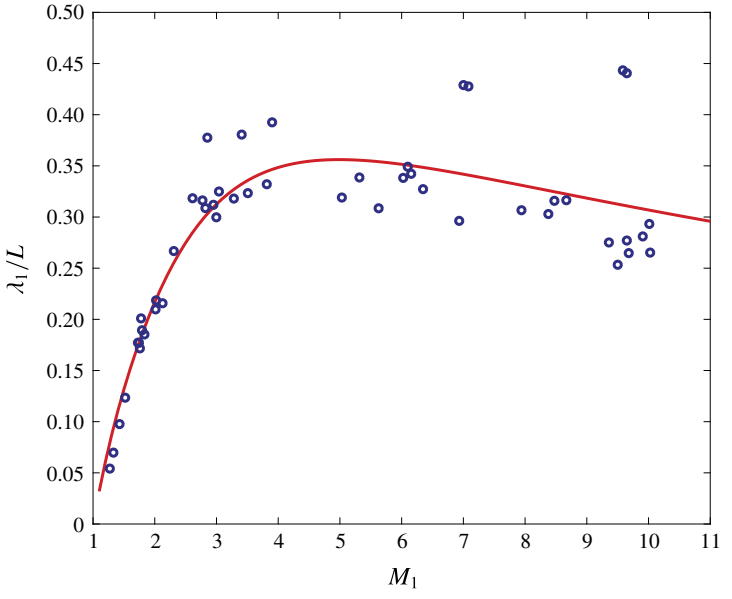


FIGURE 5. (Colour online) Inverse shock thickness, λ_1/L, as a function of upstream Mach number, M_1, in nitrogen gas: ○, experimental results of Greene & Hornig (1953), Linzer & Hornig (1963), Camac (1965), Robben & Talbot (1966) and Alsmeyer (1976); ——, present theory.

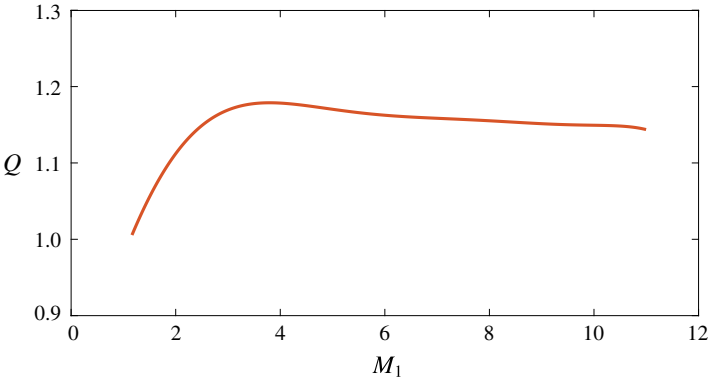


FIGURE 6. (Colour online) Asymmetry of density profiles, Q, as a function of upstream Mach number, M_1, in nitrogen gas: ——, present theory.

All terms (3) involving second derivatives result from the Knudsen number expansion and do not appear in our continuum second-order representation. We note that their presence has been recognized by Reese *et al.* (1995) as the source of oscillations in the shock structure profiles, which are not evident in experimental results.

In this work we have used standard continuum balance equations for mass, linear momentum and energy. In conjunction with the entropy inequality, we have extended

https://doi.org/10.1017/jfm.2018.291 Published online by Cambridge University Press

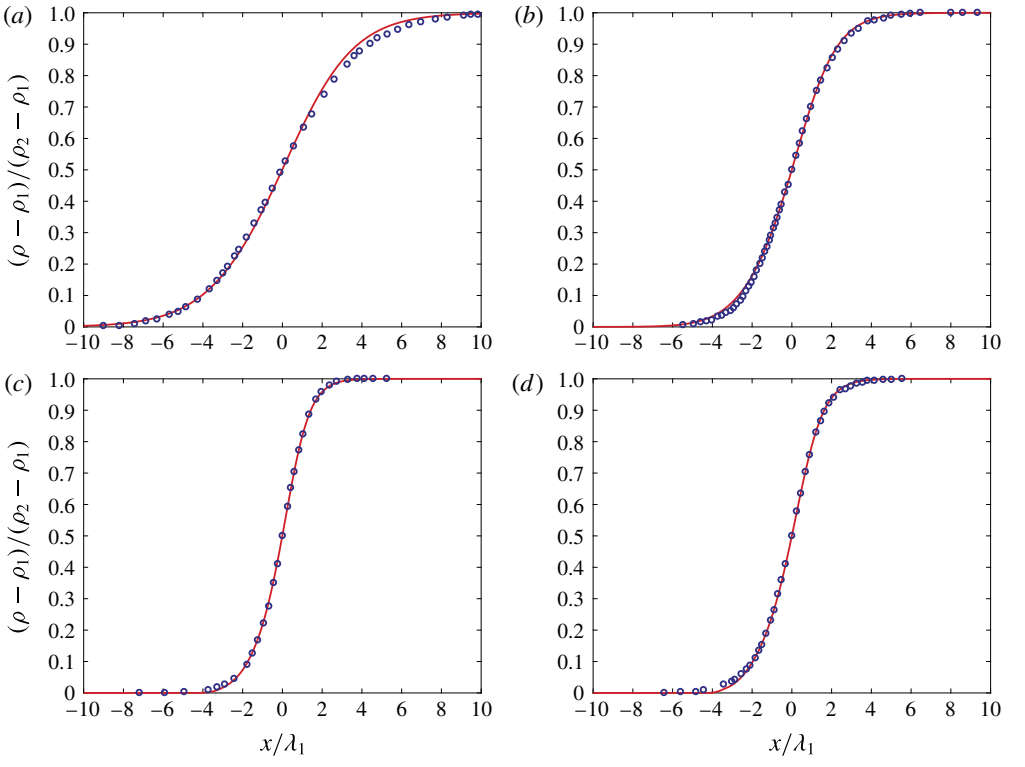


FIGURE 7. (Colour online) Shock density profiles in nitrogen gas for (*a*) $M_1 = 1.53$, (*b*) $M_1 = 2.0$, (*c*) $M_1 = 6.1$ and (*d*) $M_1 = 10.0$: ——, present theory; ○, experimental results of Alsmeyer (1976).

the constitutive equations necessitated by these equations to second order, but not in Knudsen numbers, but in strain rate and gradients of density and temperature. The solutions for the shock wave structure indicate that at higher Mach numbers our extended constitutive equations are more accurate than classical linear ones for argon and nitrogen gases. Furthermore, they are also more robust and accurate than equations obtained from expansions of the Boltzmann equation in Knudsen number or equations arising from diffusion of volume arguments.

One advantage of the present second-order constitutive relations is that, in principle, solving them should not be much more computationally expensive than solving the standard NSF equations, so complex simulations in three dimensions should be tractable. Another advantage is that these new constitutive equations reduce to the linear constitutive equations in area of low flow gradients. Therefore, the same set of equations can be applied across an entire flow field in hypersonic flow. Additional accuracy could be obtained from use of a non-ideal gas equation of state. Lastly, for application to general flows, the individual properties μ', k', k'', k''' and k'''' (as functions of ρ and θ) are required. Their experimental measurements would necessitate simple solutions of the present extended theory in cases where such properties can be clearly identified.

https://doi.org/10.1017/jfm.2018.291 Published online by Cambridge University Press

Appendix A

Recognizing that the constitutive quantities (3.3) depend on the basic fields (3.4), using the chain rule, we can write

$$\dot{\psi} = \frac{\partial \psi}{\partial \rho}\,\dot{\rho} + \frac{\partial \psi}{\partial r_i}\,\dot{r}_i + \frac{\partial \psi}{\partial D_{ij}}\,D_{ij} + \frac{\partial \psi}{\partial \theta}\,\dot{\theta} + \frac{\partial \psi}{\partial g_i}\,\dot{g}_i, \tag{A 1}$$

$$k_{i,i} = \frac{\partial k_i}{\partial \rho}\,\rho_{,i} + \frac{\partial k_i}{\partial r_j}\,r_{j,i} + \frac{\partial k_i}{\partial D_{jk}}\,D_{jk,i} + \frac{\partial k_i}{\partial \theta}\,\theta_{,i} + \frac{\partial k_i}{\partial g_j}\,g_{j,i}. \tag{A 2}$$

Substituting (A 1) and (A 2) into the Clausius–Duhem inequality (3.1), and considering that from the local mass balance (2.1) we have $\dot{\rho} = -\rho\, v_{j,j} = -\rho\, D_{jj}$ and $\dot{r}_i = -(r_j L_{ji} + \rho\, D_{ij,i} + r_i\, D_{jj})$, where $L_{ij} = D_{ij} + W_{ij}$,

$$D_{ij} = \tfrac{1}{2}(v_{i,j} + v_{j,i}) \quad \text{and} \quad W_{ij} = \tfrac{1}{2}(v_{i,j} - v_{j,i}), \tag{A 3a,b}$$

we arrive at

$$\begin{aligned}\gamma_v\theta \;=\; & -\rho\left(\eta + \frac{\partial \psi}{\partial \theta}\right)\dot{\theta} + \left[\rho\left(\rho\,\frac{\partial \psi}{\partial \rho} + r_k\,\frac{\partial \psi}{\partial \rho_k}\right)\delta_{ij} + \rho\,\frac{\partial \psi}{\partial \rho_i}\,r_j + \sigma_{ij}\right] D_{ij} \\ & - \left(\rho\,\frac{\partial \psi}{\partial r_i}\,r_j\right) W_{ij} + \left(\rho^2\,\frac{\partial \psi}{\partial r_i}\,\delta_{jk} + \theta\,\frac{\partial k_i}{\partial D_{jk}}\right) D_{jk,i} - \left(\rho\,\frac{\partial \psi}{\partial D_{ij}}\right) D_{ij} - \left(\rho\,\frac{\partial \psi}{\partial g_i}\right)\dot{g}_i \\ & + \left(\theta\,\frac{\partial k_i}{\partial \rho}\right) r_i + \left(\theta\,\frac{\partial k_i}{\partial r_j}\right) r_{j,i} + \left(\theta\,\frac{\partial k_i}{\partial g_j}\right) g_{j,i} - \left(\frac{q_i}{\theta} - \theta\,\frac{\partial k_i}{\partial \theta}\right) g_i \geqslant 0. \end{aligned} \tag{A 4}$$

Now the constitutive quantities $\{\psi,\ \eta,\ q_i,\ k_j,\ \sigma_{kl}\}$ are fixed if we fix the independent variables $\{\rho,\ \boldsymbol{r}_i,\ D_{jk},\ \theta,\ g_l\}$. Subsequently, we note that from frame invariance the constitutive quantities cannot depend on W_{ij}, and furthermore the above equation will then depend linearly on $\dot{\theta}$, D_{ik}, $\dot{g}_i$, $r_{j,i}$, $D_{ik,i}$ and $g_{j,i}$ which can still be made to vary arbitrarily and to have any sign. Thus, satisfaction of (A 4) is assured only if

$$\rho\left(\eta + \frac{\partial \psi}{\partial \theta}\right) = 0, \tag{A 5}$$

$$\rho\left(\frac{\partial \psi}{\partial r_i}\,r_j - \frac{\partial \psi}{\partial r_j}\,r_i\right) = 0, \tag{A 6}$$

$$\rho^2\,\frac{\partial \psi}{\partial r_i}\,\delta_{jk} + \theta\,\frac{\partial k_i}{\partial D_{jk}} = 0, \tag{A 7}$$

$$\rho\,\frac{\partial \psi}{\partial D_{ij}} = 0, \tag{A 8}$$

$$\rho\,\frac{\partial \psi}{\partial g_i} = 0, \tag{A 9}$$

$$\theta\left(\frac{\partial k_i}{\partial r_j} + \frac{\partial k_j}{\partial r_i}\right) = 0, \tag{A 10}$$

$$\theta\left(\frac{\partial k_i}{\partial g_j} + \frac{\partial k_j}{\partial g_i}\right) = 0, \tag{A 11}$$

https://doi.org/10.1017/jfm.2018.291 Published online by Cambridge University Press

with (A 4) reducing to

$$\gamma_v\theta = \left[\rho\left(\rho\frac{\partial\psi}{\partial\rho}+r_k\frac{\partial\psi}{\partial r_k}\right)\delta_{ij}+\rho\frac{\partial\psi}{\partial r_i}r_j+\sigma_{ij}\right]D_{ij} + \left(\theta\frac{\partial k_i}{\partial\rho}\right)r_i-\left(\frac{q_i}{\theta}-\theta\frac{\partial k_i}{\partial\theta}\right)g_i\geqslant 0. \tag{A 12}$$

In writing (A 6), (A 10) and (A 11) we have used the fact that the components of tensors W_{ij} are skew-symmetric, while those of $r_{j,i}$ and $g_{j,i}$ are symmetric.

Now, since $\rho>0$, from (A 8) and (A 9) we have that

$$\psi=\psi(\rho, r_i, \theta) \tag{A 13}$$

or, since ψ must be an isotropic function of the invariant of r_i, i.e. $I_7\equiv r_i\,r_i$, we have

$$\psi=\psi(\rho,\theta,I_7). \tag{A 14}$$

In addition, from (A 5) we have that

$$\eta=-\frac{\partial\psi}{\partial\theta}, \tag{A 15}$$

and, since $\theta>0$, from (A 7) that

$$k_i=\widehat{k}_i-\frac{\rho^2}{\theta}\frac{\partial\psi}{\partial r_i}D_{kk}, \tag{A 16}$$

where $\widehat{k}_i$ is independent of D_{jk}. Substituting (A 14) and (A 16) into (A 10) we obtain

$$\theta\left(\frac{\partial\widehat{k}_i}{\partial r_j}+\frac{\partial\widehat{k}_j}{\partial r_i}\right)-2\rho^2\frac{\partial^2\psi}{\partial r_i\partial r_j}D_{kk}=0. \tag{A 17}$$

Now since ψ and $\widehat{k}_i$ are independent of D_{jk}, we must have that

$$\frac{\partial^2\psi}{\partial r_i\partial r_j}=0 \quad\text{and}\quad \frac{\partial\widehat{k}_i}{\partial r_j}+\frac{\partial\widehat{k}_j}{\partial r_i}=0. \tag{A 18a,b}$$

It subsequently follows from (A 14), (A 16) and (A 18) that

$$\psi=\psi\,(\rho,\theta)\quad\text{and thus}\quad k_i=\widehat{k}_i. \tag{A 19a,b}$$

It now remains to exploit (A 10) and (A 11) and recall that k_i is independent of D_{jk}. We first note that both equations are of the form

$$\frac{\partial f_i}{\partial y_j}+\frac{\partial f_j}{\partial y_i}=0 \tag{A 20}$$

whose general solution is given by

$$f_i=a_i+A_{ij}\,y_j, \tag{A 21}$$

where A_{ij} is skew-symmetric, and both a_i and A_{ij} are independent of y_k.

Now, from (A 10) we have that

$$k_i=a_i+A_{ij}\,r_j, \tag{A 22}$$

https://doi.org/10.1017/jfm.2018.291 Published online by Cambridge University Press

where A_{ij} is skew-symmetric and both a_i and A_{ij} are independent of r_k. Substituting (A 22) into (A 11) we obtain

$$\left(\frac{\partial a_i}{\partial g_k}+\frac{\partial a_k}{\partial g_i}\right)+\left(\frac{\partial A_{ij}}{\partial g_k}+\frac{\partial A_{kj}}{\partial g_i}\right) r_j = 0. \tag{A 23}$$

It follows that

$$\frac{\partial a_i}{\partial g_k}+\frac{\partial a_k}{\partial g_i}=0 \quad \text{and} \quad \frac{\partial A_{ij}}{\partial g_k}+\frac{\partial A_{kj}}{\partial g_i}=0. \tag{A 24a,b}$$

Subsequently,

$$a_i = b_i + B_{ij}\, g_j \quad \text{and} \quad A_{ij} = c_{ij} + C_{ijk}\, g_k, \tag{A 25a,b}$$

where B_{ij} and c_{ij} are skew-symmetric, C_{ijk} is completely skew-symmetric and b_i, B_{ij}, c_{ij} and C_{ijk} are independent of g_l, or more appropriately, they are only functions of ρ and θ. Substituting (A 25) into (A 22) we have

$$k_i = b_i + c_{ij}\, r_j + B_{ij}\, g_j + C_{ijk}\, r_j\, g_k. \tag{A 26}$$

However, there are no objective isotropic tensors of ranks 1, 2 and 3 that are only functions of the scalars ρ and θ. Subsequently, $b_i = c_{ij} = B_{ij} = C_{ijk} = 0$ and thus $k_i = 0$, or from (3.2)

$$h_i = \frac{q_i}{\theta}. \tag{A 27}$$

Lastly, we note that the reduced entropy inequality (A 12) reduces to

$$\gamma\,\theta = \left(\rho^2\,\frac{\partial \psi}{\partial \rho}\,\delta_{ij}+\sigma_{ij}\right) D_{ij} - \frac{q_i}{\theta}\, g_i \geqslant 0. \tag{A 28}$$

REFERENCES

ALSMEYER, H. 1976 Density profiles in argon and nitrogen shock waves measured by the absorption of an electron beam. *J. Fluid Mech.* **74** (3), 497–513.

BALAKRISHNAN, R. 2004 An approach to entropy consistency in second-order hydrodynamic equations. *J. Fluid Mech.* **503**, 201–245.

BALAKRISHNAN, R. & AGARWAL, R. K. 1999 A comparative study of several higher-order kinetic formulations beyond Navier–Stokes for computing the shock structure. In *37th AIAA Aerospace Sciences Meeting and Exhibit*, AIAA-99-0224. American Institute of Aeronautics and Astronautics.

BIRD, G. A. 1970 Aspects of the structure of strong shock waves. *Phys. Fluids* **13** (5), 1172–1177.

BRAU, C. A. 1967 Kinetic theory of polyatomic gases: models for the collision processes. *Phys. Fluids* **10**, 48–55.

BRENNER, H. 2005*a* Kinematics of volume transport. *Physica* A **349** (1–2), 11–59.

BRENNER, H. 2005*b* Navier–Stokes revisited. *Physica* A **349** (1–2), 60–132.

CAMAC, M. 1965 Argon and nitrogen shock thicknesses. In *Proceedings of the Fourth International Symposium on Rarefied Gas Dynamics* (ed. J. H. de Leeuw), vol. 1, p. 240. Academic Press.

CHAPMAN, S. & COWLING, T. G. 1970 *The Mathematical Theory of Non-Uniform Gases*. Cambridge University Press.

https://doi.org/10.1017/jfm.2018.291 Published online by Cambridge University Press

CHEN, J. 2013 Extension of nonlinear Onsager theory of irreversibility. *Acta Mechanica* **224**, 31533158.

COLEMAN, B. D., MARKOVITZ, H. & NOLL, W. 1966 *Viscometric Flows of Non-Newtonian Fluids*. Springer.

COLEMAN, B. D. & NOLL, W. 1961 Foundations of linear viscoelasticity. *Rev. Mod. Phys.* **33** (2), 239–249.

COMEAUX, K. A., CHAPMAN, D. R. & MACCORMACK, R. W. 1995 An analysis of the Burnett equations based on the second law of thermodynamics. In *33rd AIAA Aerospace Sciences Meeting and Exhibit*, AIAA-95-0415. American Institute of Aeronautics and Astronautics.

ERINGEN, A. C. 1980 *Mechanics of Continua*. Krieger.

ERINGEN, A. C. 1999 *Microcontinuum Field Theories I: Foundations and Solids*. Springer.

ERINGEN, A. C. 2001 *Microcontinuum Field Theories II: Fluent Media*. Springer.

GAREN, W., SYNOFZIK, R. & FROHN, A. 1974 Shock-tube for generating weak shock-waves. *AIAA J.* **12** (8), 1132–1134.

GILBARG, D. 1951 The existence and limit behavior of the one-dimensional shock layer. *Am. J. Maths* **73** (2), 256–274.

GILBARG, D. & PAOLUCCI, D. 1953 The structure of shock waves in the continuum theory of fluids. *J. Ration. Mech. Anal.* **2** (4), 617–642.

GRAD, H. 1949 On the kinetic theory of rarefied gases. *Commun. Pure Appl. Maths* **2** (4), 331–407.

GRAD, H. 1952 The profile of a steady plane shock wave. *Commun. Pure Appl. Maths* **5** (3), 257–300.

GREENE, E. F. & HORNIG, D. F. 1953 The shape and thickness of shock fronts in argon, hydrogen, nitrogen, and oxygen. *J. Chem. Phys.* **21** (4), 617–624.

GREENSHIELDS, C. J. & REESE, J. M. 2007 The structure of shock waves as a test of Brenner's modifications to the Navier–Stokes equations. *J. Fluid Mech.* **580**, 407–429.

JIN, S & SLEMROD, M 2001 Regularization of the Burnett equations via relaxation. *J. Stat. Phys.* **103** (5–6), 1009–1033.

KHONKIN, A. D. & ORLOV, A. V. 1993 Weak shock structure on the basis of modified hydrodynamical equations. *Phys. Fluids* A **5** (7), 1810–1813.

LANDAU, L. D. & LIFSHITZ, E. M. 1959 *Fluid Mechanics*, Course of Theoretical Physics, vol. 6. Pergamon Press.

LIEPMANN, H. W., NARASIMHA, R. & CHAHINE, M. T. 1962 Structure of a plane shock layer. *Phys. Fluids* **5** (11), 1313–1324.

LINZER, M. & HORNIG, D. F. 1963 Structure of shock fronts in argon and nitrogen. *Phys. Fluids* **6** (12), 1661–1668.

LIU, I.-S. 2002 *Continuum Mechanics*. Springer.

LIU, I.-S. & SALVADOR, J. A. 1990 Hyperbolic system for viscous fluids and simulation of shock tube flows. *Contin. Mech. Thermodyn.* **2** (3), 179–197.

LUDFORD, G. S. S. 1951 The classification of one-dimensional flows and the general shock problem of a compressible, viscous, heat-conducting fluid. *J. Aero. Sci.* **18** (12), 830–834.

LUMPKIN, F. E. & CHAPMAN, D. R. 1992 Accuracy of the Burnett equations for hypersonic real gas flows. *J. Thermophys. Heat Transfer* **6** (3), 419–425.

VON MISES, R. 1950 On the thickness of a steady shock wave. *J. Aero. Sci.* **17** (9), 551–554; 594.

MORDUCHOW, M. & LIBBY, P. A. 1949 On a complete solution of the one-dimensional flow equations of a viscous, heat-conducting, compressible gas. *J. Aero. Sci.* **16** (11), 674–684; 704.

PAOLUCCI, S. 2016 *Continuum Mechanics and Thermodynamics of Matter*. Cambridge University Press.

REESE, J. M., WOODS, L. C., THIVET, F. J. P. & CANDEL, S. M. 1995 A second-order description of shock structure. *J. Comput. Phys.* **117** (2), 240–250.

RIEUTORD, E. 1970 Contribution à l'étude de l'onde de choc primaire en tube à choc. PhD thesis, Institut National des Sciences Appliquées de Lyon.

ROBBEN, F. & TALBOT, L. 1966 Measurement of shock wave thickness by electron beam fluorescence method. *Phys. Fluids* **9** (4), 633–643.

https://doi.org/10.1017/jfm.2018.291 Published online by Cambridge University Press

RUSSELL, D. 1965 In *Proceedings of the Fourth International Symposium on Rarefied Gas Dynamics* (ed. J. H. de Leeuw), vol. 1, p. 265. Academic Press.

SALOMONS, E. & MARESCHAL, M. 1992 Usefulness of the Burnett description of strong shock waves. *Phys. Rev. Lett.* **69** (2), 269–272.

SCHMIDT, B. 1969 Electron beam density measurements in shock waves in argon. *J. Fluid Mech.* **39** (2), 361–373.

SCHULTZ-GRUNOW, F. & FROHN, A. 1965 In *Proceedings of the Fourth International Symposium on Rarefied Gas Dynamics* (ed. J. H. de Leeuw), vol. 1, p. 250. Academic Press.

SHE, R. S. & SATHER, N. F. 1967 Kinetic theory of polyatomic gases. *J. Chem. Phys.* **47**, 4978–4993.

SHERMAN, F. S. 1955 A low-density wind-tunnel study of shock-wave structure and relaxation phenomena in gases. *NACA Technical Note* 3298. National Advisory Committee for Aeronautics.

STRUCHTRUP, H. & TORRILHON, M. 2003 Regularization of Grad's 13 moment equations: derivation and linear analysis. *Phys. Fluids* **15** (9), 2668–2680.

TANIGUCHI, S., ARIMA, T., RUGGERI, T. & SUJIYAMA, M. 2014*a* Shock wave structure in a rarefied polyatomic gas based on extended thermodynamics. *Acta Appl. Maths* **132** (1), 583–593.

TANIGUCHI, S., ARIMA, T., RUGGERI, T. & SUJIYAMA, M. 2014*b* Thermodynamic theory of the shock wave structure in a rarefied polyatomic gas: beyond the Bethe–Teller theory. *Phys. Rev.* E **89**, 013025.

THOMAS, L. H. 1944 Note on Becker's theory of the shock front. *J. Chem. Phys.* **12** (11), 449–453.

TRUESDELL, C. & NOLL, W. 2004 *Non-linear Field Theories of Mechanics*, 3rd edn. Springer.

WEISS, W. 1995 Continuous shock structure in extended thermodynamics. *Phys. Rev.* E **52** (6), R5760–R5763.

WOODS, L. C. 1983 Frame-indifferent kinetic theory. *J. Fluid Mech.* **136**, 423–433.

WOODS, L. C. 1993 *An Introduction to the Kinetic Theory of Gases and Magnetoplasmas*. Oxford University Press.

ZHENG, Q.-S. 1993 On the representations for isotropic vector-valued, symmetric tensor-valued and skew-symmetric tensor-valued functions. *Intl J. Engng Sci.* **31** (7), 1013–1024.

ZHENG, Q.-S. 1994 Theory of representations for tensor functions: a unified invariant approach to constitutive equations. *Appl. Mech. Rev.* **47** (11), 545–587.

https://doi.org/10.1017/jfm.2018.291 Published online by Cambridge University Press